

Received October 20, 2019, accepted November 5, 2019, date of publication November 11, 2019, date of current version November 20, 2019.

Digital Object Identifier 10.1109/ACCESS.2019.2952613

# Development of an Online Home Appliance Control System Using Augmented Reality and an SSVEP-Based Brain-Computer Interface

SEONGHUN PARK<sup>1</sup>, HO-SEUNG CHA<sup>1</sup>, AND CHANG-HWAN IM<sup>1</sup>, (Member, IEEE)

Department of Biomedical Engineering, Hanyang University, Seoul 04763, South Korea

Corresponding author: Chang-Hwan Im (ich@hanyang.ac.kr)

This work was supported in part by the National Research Foundation of Korea (NRF) under Grant 2019R1A2C2086593 and in part by the Institute for Information and communications Technology Promotion (IITP) funded by the Korean Government (MSIT) under Grant 2017-0-00432 (Development of Non-Invasive Integrated BCI SW Platform to Control Home Appliances and External Devices by user's thought via AR/VR interface).

**ABSTRACT** In this study, we implemented a new home appliance control system by combining electroencephalography (EEG)-based brain-computer interface (BCI), augmented reality (AR), and internet of things (IoT) technologies. We adopted a steady-state visual evoked potential (SSVEP)-based BCI paradigm for the implementation of a fast and robust BCI system. In the offline experiment, we compared the performances of three BCIs adopting different types of visual stimuli in an AR environment to determine the optimal visual stimulus. In the online experiment, we evaluated the feasibility of the proposed smart home system using the optimal stimulus by controlling three home appliances in real time. The visual stimuli were presented on a see-through head-mounted display (HMD), while the recorded brain activity was analyzed to classify the control command, and the home appliances were controlled through IoT. In the offline experiment, a grow/shrink stimulus (GSS) consisting of a star-shaped flickering object of varying size was selected as the optimal stimulus, eliciting SSVEP responses more effectively than the other options. In the online experiment, all users could turn the BCI-based control system on/off whenever they wanted using the eye-blinking-based electrooculogram (EOG) switch, and could successfully perform all the designated control tasks without difficulty. The average classification accuracy of the SSVEP-BCI-based control system was 92.8%, with an information transfer rate (ITR) of 37.4 bits/min. The proposed system exhibited an excellent performance, surpassing the best results reported in previous studies regarding external device control based on BCI using an HMD as rendering device.

**INDEX TERMS** Augmented reality, brain-computer interface, electroencephalography, internet of things, steady-state visual evoked potential.

## I. INTRODUCTION

Brain-computer interface (BCI) is a technology that provides a direct communication channel between a user and the external environment using the user's brain activity [1]–[4]. Several noninvasive techniques have been utilized to record the brain activity of users, including near-infrared spectroscopy (fNIRS), magnetoencephalography (MEG), and electro-encephalography (EEG). Among these, EEG has been the most widely employed modality, because it is affordable, easy to use, and portable. EEG-based BCIs have been

intensively developed for a variety of applications, such as communication [5]–[7], rehabilitation [8], [9], entertainment [10], and control of electric devices [11]–[14].

Recently, as the number of people with disability and elderly people who require special care in daily life activities have rapidly increased [15], [16], the necessity of developing “smart home” systems tailored for such people has arisen. In line with this trend, the implementation of home automation systems using BCI technology has drawn increasing interest [17]. For example, Takano *et al.* developed a home appliance control system with an infrared remote controller and augmented-reality head-mounted display (AR-HMD) based on a P300-based BCI [18]. Wolpaw *et al.* were the

The associate editor coordinating the review of this manuscript and approving it for publication was Mohammad Zia Ur Rahman<sup>1</sup>.

first to attempt to implement an AR-based home automation system. However, the information transfer rate (ITR) [19] of the BCI system was not sufficiently high for utilization in practical scenarios (ITR = 5.4 bits/min), owing to the low signal-to-noise ratio of the P300 component. A BCI system based on steady-state visual evoked potential (SSVEP), a periodic brain response evoked by the presentation of a visual stimulus flickering or reversing at a specific frequency, can also be used to implement an external device control system. Recently, Lo *et al.* implemented an external device control system that can be potentially used in hospitals [12] using SSVEP-based BCI because it is well known that an SSVEP-based BCI exhibits a stronger performance than a P300-based BCI in terms of the ITR and robustness [6], [20]. However, Lo *et al.* employed a relatively “bulky” LCD monitor as the rendering device to present visual stimuli, constraining the flexibility and mobility of the BCI-based home automation system in real-world scenarios. Indeed, although using an AR-HMD as the rendering device can provide a potential solution to this problem, no previous study on SSVEP-based home appliance control systems has employed an AR-HMD to present visual stimuli.

On the other hand, investigating the feasibility of employing an AR-HMD for SSVEP-based home appliance control systems is important, because the low contrast ratio of AR-HMDs weakens the contrast between the visual stimuli and the background, possibly degrading the overall performance of the BCI system [21], [22]. Note that typical LCD monitors have a contrast ratio of 1:1,000 or higher, while AR-HMDs have a contrast ratio lower than 1:400 [21].

In the present study, we investigated whether an SSVEP-based home appliance control system with AR-HMDs exhibits a sufficiently strong performance for utilization in practical scenarios. To determine the optimal visual stimulus that maximizes the performance of an AR-HMD-based BCI system, various types of visual stimuli eliciting SSVEP responses were tested. We then implemented an online home appliance control system by incorporating an AR-based BCI system with the optimal visual stimulus. Then, internet of things (IoT) technology was employed to enable wireless communications among devices. The performance of the developed smart home system was evaluated using online experiments with a number of healthy participants wearing AR-HMDs, where three home appliances were controlled in real time.

## II. METHODS

### A. EXPERIMENT I – OFFLINE EXPERIMENT TO DETERMINE OPTIMAL VISUAL STIMULI

#### 1) SUBJECTS

Twenty-one healthy adults (13 males and eight females, aged  $23.3 \pm 2.7$  years) with normal or corrected-to-normal vision participated in our experiments; however, the data of one participant were excluded in the further analysis because no spectral peak was observed at any SSVEP frequency

(see Fig. S1 in the Supplementary Information file), and thereby EEG data of 20 participants were analyzed in the further analysis. This so-called “BCI-illiteracy” is a well-known issue in EEG-based BCI [23]. All participants were informed of the details of the experiments and provided written consent. This study and the experimental paradigm were approved by the institutional review board of Hanyang University, Republic of Korea (IRB No. HYI-14-167-11).

#### 2) VISUAL STIMULI FOR SSVEP-BASED BCI

In this study, three different types of visual stimuli were tested under an AR environment: 1) pattern-reversal checkerboard stimulus (PRCS), 2) flicker stimulus (FS), and 3) grow and shrink stimulus (GSS). All the visual stimuli were presented on the see-through display of an MS Hololens™ (Microsoft, Company, Redmond, WA, USA). An additional PRCS stimulus (LCD-PRCS) was presented on an LCD monitor as the reference of a typical SSVEP visual stimulus, resulting in four types of stimuli in total (Fig. 1). PRCS is a widely employed visual stimulus to elicit SSVEP responses, where the checkerboard pattern is reversed at a constant frequency [20], [24], [25]. FS is another commonly used visual stimulus, which elicits SSVEP responses by changing the luminance of the stimulus at a constant frequency [26]. Unlike PRCS and FS, which change the contrast or luminance of the visual stimulus, the proposed GSS stimulus changes its size and luminance concurrently to elicit SSVEP responses. It has recently been reported that periodic motion of a visual stimulus can also elicit a periodic VEP response, similar to the conventional SSVEP responses [27]–[29]. This is often referred to as the “steady-state motion visual evoked potential (SSMVEP)” [29]. Our GSS stimulus not only changes its size from small to large (grow) and back to small (shrink) at a constant frequency, but also flickers at the same frequency (please watch the attached Supplementary movie or visit a

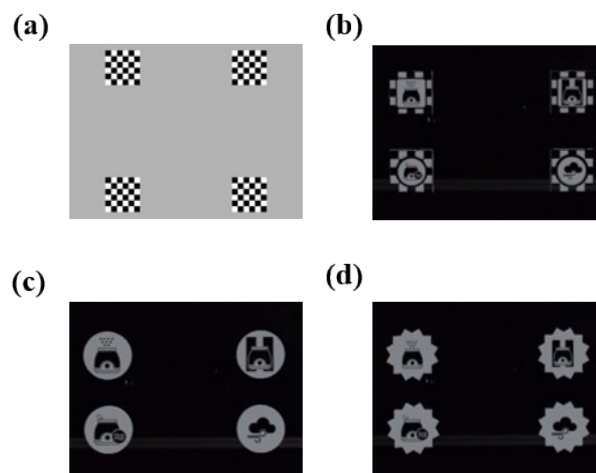


**FIGURE 1.** The stimuli used in the offline experiment (Experiment I). (a) LCD-PRCS, (b) PRCS, (c) FS, and (d) GSS. Note that only LCD-PRCS was presented on an LCD screen, while the others were presented on a see-through AR display.

YouTube link [30] for higher quality video, which was taken during the online experiment).

For each of three visual stimulus types, four stimuli with different frequencies (7.5, 8.57, 10 and 12 Hz) were generated. These frequencies were selected considering the refresh rate of the rendering device and previous studies that investigated the relationship between stimulation frequency and SSVEP responses [31], [32]. Note that both the HoloLens and LCD monitor had the same refresh rate of 60 Hz, which is an integer multiple of the four target frequencies.

### 3) EXPERIMENTAL PARADIGM

The offline experiment consisted of four sessions to test the four different stimulus types (PRCS, FS, GSS, and LCD-PRCS). In each block, a randomly selected type of stimuli was presented. Each session consisted of 20 trials, each of which lasted for 5 s with a 2-s inter-stimulus interval (ISI). In each trial, four visual stimuli with different frequencies were presented (see Fig. 1), and the participant was instructed to remain focused on one of these without eye blinks and body movements. The participant rested for at least 3 min between consecutive blocks, to avoid eye fatigue.

A reference stimulus, called LCD-PRCS, was presented on a 24-inch LCD monitor with a resolution of  $1920 \times 1080$  pixels, and the distance between the participant and the monitor was maintained at 60 cm. The visual angle between the center of the screen and each stimulus was set to  $5.6^\circ$ , and the same visual angle was also applied to the visual stimuli presented on the see-through HoloLens display.

The visual stimuli on the LCD monitor were generated and controlled using Cogent Graphics and the Cogent2000 Toolbox [33]. The visual stimuli in the AR environment were controlled using an in-house program developed with Unity (Unity Technologies ApS, San Francisco, CA, USA), and a UDP communication program developed using C#.

### 4) DATA RECORDING AND PREPROCESSING

The EEG data were recorded at a 2,048 Hz sampling rate from 33 electrodes (Fp1, Fp2, AF3, AF4, F7, F3, Fz, F4, F8, FC5, FC1, FC2, FC6, T7, C3, Cz, C4, T8, CP5, CP1, CP2, CP6, P7, P3, Pz, P4, P8, PO3, POz, PO4, O1, Oz, and O2) attached to the scalp surface, using the BioSemi ActiveTwo system (Biosemi, Amsterdam, The Netherlands). A CMS active electrode and a DRL passive electrode were used to form a feedback loop for the amplifier reference. Details of the feedback loop can be found at [34]. The recorded EEG data were down-sampled to 512 Hz to reduce the computational cost, and then re-referenced to Cz. To remove low frequency drift and power line noise (60 Hz), the re-referenced data were band-pass filtered with 2 and 54 Hz cutoff frequencies, using a zero-phase Butterworth infinite impulse response filter implemented in MATLAB (MathWorks, Inc., Natick, MA, USA). We confirmed that the orders of re-referencing and bandpass filtering did not affect the EEG signal-to-noise ratio.

### 5) DATA ANALYSIS

For the classification of SSVEP responses recorded while a participant was viewing a specific visual stimulus, a recently developed algorithm called the multivariate synchronization index (EMSI) [35] was adopted. EMSI first calculates the synchronizations between a given EEG signal and reference signals generated with stimulation frequencies and their harmonics, and then finds a specific stimulation frequency that maximizes the synchronization index. More detailed explanations on the EMSI algorithm can be found in [35]. In this study, three harmonic frequencies were taken into account.

To determine the optimal duration of the visual stimuli presentation, we evaluated the ITR with respect to the different window sizes based on the following formula:

$$ITR = \frac{60}{T} (\log_2 N + P \log_2 P + (1 - P) \log_2 (\frac{1 - P}{N - 1})), \quad (1)$$

where T represents the window size, N denotes the number of possible targets and P is the classification accuracy.

In the data analysis, an electrode set consisting of O1, Oz, and O2 was tested to investigate whether the proposed system can achieve feasible performance with an electrode set having been typically used in SSVEP-based BCI studies. Conversely, we also calculated the classification accuracies for all possible combinations of three electrodes out of the nine electrodes attached above the Occipital lobe (P7, P3, Pz, P4, P8, PO3, POz, PO4, O1, Oz, and O2) and selected the three electrodes that exhibited the highest classification accuracy for each participant. We then compared the highest individual classification accuracies of the four SSVEP stimuli types. The individually selected electrode sets were employed in the following online home appliance control experiments.

### 6) STATISTICAL ANALYSIS

Because the testing dataset did not follow a normal distribution according to the Kolmogorov-Smirnov test, the Friedman and Wilcoxon signed rank tests were performed to test the statistical significance. The significance level for the Friedman test was set to 0.05, and a Bonferroni-corrected Wilcoxon signed rank post-hoc analysis was employed to test the statistical significance.

## B. EXPERIMENT II – ONLINE HOME APPLIANCE CONTROL EXPERIMENT

### 1) SUBJECTS

Although we attempted to enroll all the participants who participated in the offline experiment again for the online experiment, three of the 20 participants were unable to participate because of personal reasons (e.g., leave of absence for a full semester). Consequently, 17 participants took part in the online experiment.

### 2) SELF-REGULATING ON/OFF SWITCH

For the participants to switch the home appliance control system on/off by themselves, an eye blink-based switch was adopted. For the accurate detection of eye blinks,

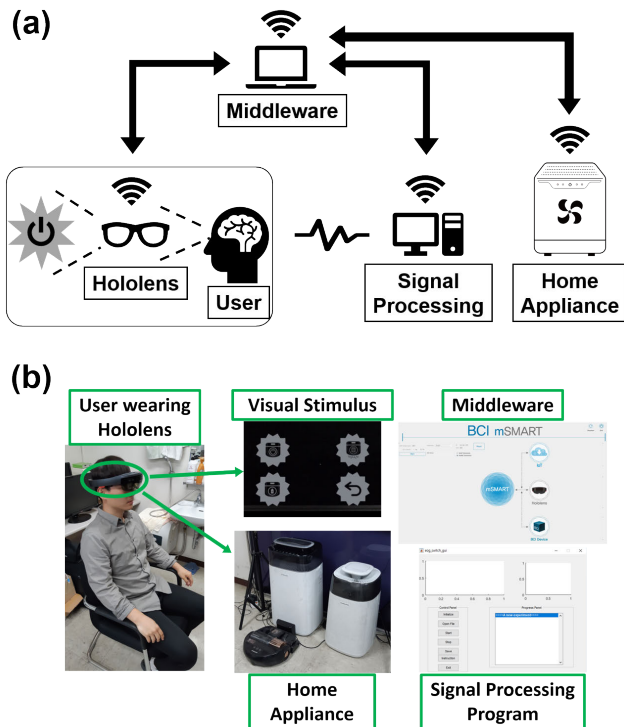


**FIGURE 2.** (a) A schematic diagram of the proposed home appliance control system. The visual stimuli were presented to the user via a Hololens, which was controlled by the middleware. The physiological signals recorded from the user were analyzed by real-time signal processing software, and then sent to the middleware. Based on the analysis results, the middleware generated an appropriate command and delivered this to the selected home appliance. The experiment was conducted in an environment in which the Hololens, middleware, signal processing program, and home appliances were all connected to the same Wi-Fi network. (b) Real pictures of the developed platform.

a recently developed method called multiple-window summation of first derivatives in a sliding window (MSDW) was adopted [36]. An electrooculogram (EOG) signal recorded from the Fp1 channel was utilized. When a participant blinked their eyes more than four times within 3 s, the home appliance control system was switched on (or off).

### 3) EXPERIMENTAL PARADIGM

A schematic diagram of the proposed home appliance control system is presented in Fig. 2. We developed a program called “middleware” to mediate the communication between the Hololens, signal processing software in MATLAB, IoT-based device control software, and IoT-supported home appliances. Three home appliances were controlled in this experiment: a robotic vacuum, air cleaner, and humidifier. The device control software was developed using the Samsung IoT device control API (Samsung Electronics, Company, Ltd., Seoul, South Korea), as all the home appliances were Samsung products. The device control software was merged with the middleware.

The proposed home appliance control system consisted of two stages: “device selection” and “command selection.” The hierarchical constitution of the system and the stimuli employed in the experiment is illustrated in Fig. 3. Once a

participant switched on the system by repeatedly blinking, four visual stimuli were presented on the AR display. In this “device selection” stage, three stimuli were assigned to three different home appliances, and the other stimulus was assigned to the “EXIT” function. Each stimulus was represented by intuitive icons, as depicted in Fig. 3b. Once the target device was selected based on the SSVEP responses, the middleware made the Hololens present a new set of visual stimuli, through which detailed device control was possible (see Fig. 3c, 3d, and 3e). In this “command selection” stage, four SSVEP stimuli with three icons representing different control commands and one “back to the previous step” icon were presented. Participants were able to control a pre-selected device by looking at the command stimuli, or to go back to the previous “device selection” stage by looking at the “back to the previous step” icon. Furthermore, the participants could turn off the system either by looking at the “EXIT” icon in the “device selection” stage or repeatedly blinking their eyes again anytime during the system operation. The time assigned for each selection trial was fixed to 2.5 s.

In the “device selection” stage, the ISI was fixed to 1 s. In the “command selection” stage, the first ISI was set to 1 s, and the following ISIs were set to 4 s, to allow the participants time to confirm whether the device operated correctly according to their intentions. In the “command selection” stage, the participants were able to run four different commands including “back to the previous step” (see Table 1). For example, when a participant selected the robotic vacuum in the “device selection” stage, they could turn on the vacuum and then execute “turbo mode” by consecutively selecting the second and third stimuli. If the system misidentified the participant’s intention, then they could select the “back to the previous step” command to return to the previous selection step.

Before the main experiment, each participant was given 10–20 min to become accustomed to the BCI-based device control system. The experiment started when the participant announced that they completely understood the system and

**TABLE 1.** The presented commands of each home appliance in ‘Command Selection’ stage.

Home Appliance	Commands			
Robotic Vacuum	On/Off (Toggle*)	Turbo Mode	Charge	Back
Air Cleaner	On/Off (Toggle*)	Auto-wind Mode	Sleep Mode	Back
Humidifier	On/Off (Toggle*)	Auto-wind Mode	Sleep Mode	Back

\* Note that the icon for turning on/off each device was functioned as a toggle switch, according to the device status

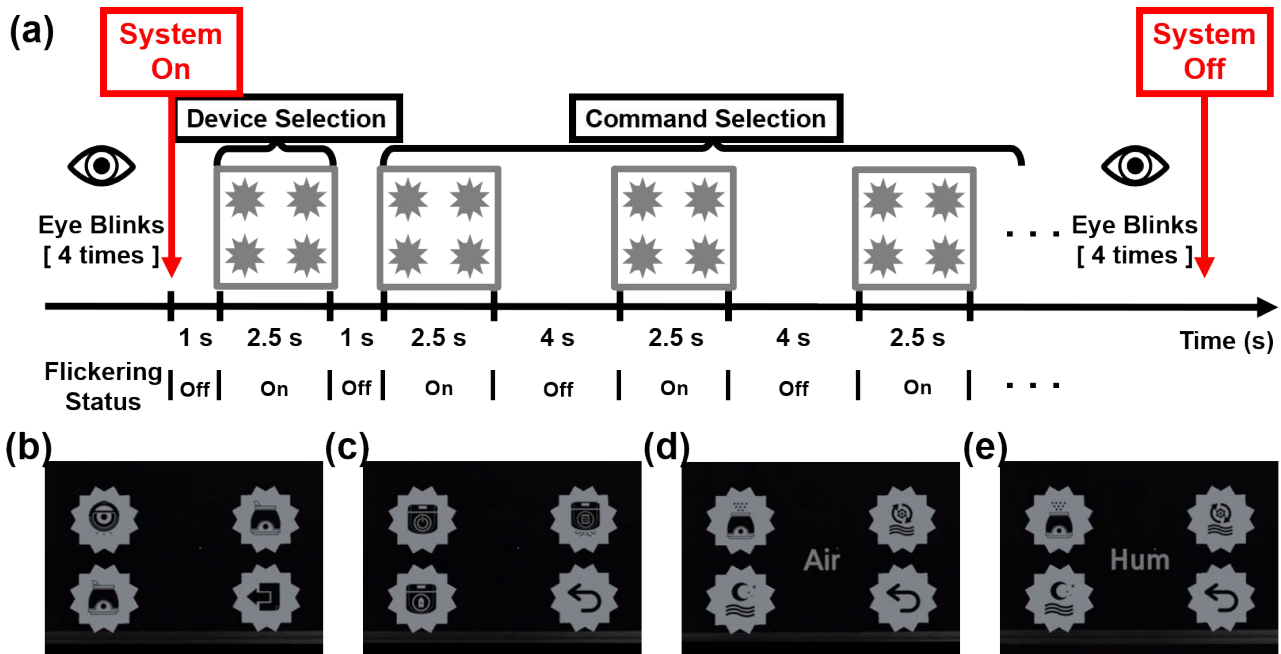


**FIGURE 3.** Overall procedure of the online experiment (Experiment II). (a) The hierarchical constitution of the proposed home appliance control system. Repeated eye blinks start the control system. After delivering a designated command to a selected home appliance, the control system is turned off by repeated eye blinks of the user. (b) The visual stimuli presented in the “device selection” stage. (c), (d), and (e) show the visual stimuli presented in the “command selection” stage to control the robotic vacuum, air cleaner, and humidifier, respectively.

were fully ready to use the system. There were two different experimental sessions with different scenarios, referred to as single-command and multicommand sessions. In the single-command session, the participants were instructed to turn on the system, execute a single pre-instructed command, and then turn off the system. This process was defined as one block. Instructions were provided to the participants before starting each block. The participants were asked to execute all commands for each device, resulting in 12 blocks (three devices × four commands) in the single-command session. If a participant made a mistake or the classifier misidentified the participant’s intention, then he or she had to correct the wrong operation and then conduct the pre-instructed task again to complete the block. For example, assume that the given instruction is to select a robotic vacuum and execute “turbo mode.” If the robotic vacuum was turned off either through a mistake by the participant or a misclassification, then the participant could turn it on by looking at the “ON/OFF” icon and then look at the “turbo mode” icon again to complete the task. As another example, if the participant was pre-instructed to select “air cleaner” but “humidifier” was selected, they could go back to the previous “device selection” stage by looking at “back to the previous step” icon and focus on the “air cleaner” icon again. Otherwise, they could turn off the whole system and turn it on again by blinking repeatedly and then select the “air cleaner” in the “device selection” stage. The participants could tackle this situation according to their own preferences.

In the multicommand session, each block consisted of turning on a designated device, executing four different commands consecutively, and turning off the device, resulting in three blocks (three devices). The order of executing commands was predefined and communicated to the participants before starting each block. As in the single-command session, the participants needed to correct errors (misclassifications) occurring during the task using their own approach.

In this study, a “trial” was defined as a single presentation of visual stimuli. For example, in the single-command session the minimum number of trials required to complete a task (one block) was two (one trial for “device selection” and the other trial for “command selection” in the case where there was no error). Therefore, to complete the single-command session, at least 24 trials (three devices × two stages × four commands) were required. Likewise, to complete the multicommand session, at least 15 trials (three devices × (one “device selection” + four “command selection”)) were required.

Between two successive sessions, participants watched three video clips for approximately 12 min to investigate the time required to operate the eye-blink-based switch and evaluate the false positive rate (FPR) of this operation. The participants were instructed to repetitively blink their eyes to operate the eye-blink-based switch at a random time communicated by the experimenter for each video, when the switch did not actually work: The experimenter paused the video and asked the participants to blink their eyes. Once the eye blink detection algorithm successfully detected more than four eye

blinks within 3 s, the experimenter played the video again. At the end of each video, the participants were instructed to repetitively blink their eyes once again.

#### 4) DATA RECORDING AND ANALYSIS

Based on the results of the offline experiments, the three electrodes that yielded the highest classification accuracy for each participant were selected for the online experiments. All the preprocessing and SSVEP classification methods were the same as in the offline experiments. The Wilcoxon signed rank test was utilized to test the statistical significance between the performances in both experiments, as the dataset did not follow a normal distribution. In addition to classification accuracy and ITR, efficiency was also calculated to evaluate the actual availability of the proposed system. Efficiency considers not only the classification accuracy of the system, but also the cost to correct errors occurred by misclassification. An efficiency equal to 1 represents that no error occurred during the system operation (ideal case), while an efficiency close to 0 implies that the system is affected by errors so severely that the performance measures including ITR and classification accuracy may not be meaningful.

### III. RESULTS

#### A. EXPERIMENT I – OFFLINE EXPERIMENT TO DETERMINE OPTIMAL VISUAL STIMULI

To determine the optimal visual stimulus for an SSVEP-based BCI in an AR environment, we first evaluated the classification accuracy for each stimulus type when the same universal electrodes (O1, Oz, and O2) were used for each participant. The averaged accuracies with respect to different window sizes are shown in Fig. 4. For every window size, GSS exhibited the best performance in terms of the classification accuracy, followed by FS and PRCS. The Friedman

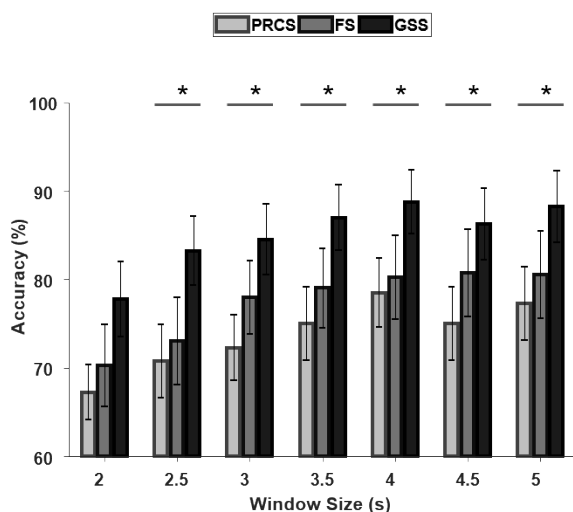


**FIGURE 4.** Comparison of the mean classification accuracy for the three visual stimuli in the AR environment when the universal electrode configuration was used (O1, Oz, and O2). Error bars indicate the standard errors across the participants (\* represents Bonferroni-corrected  $p < 0.05$ ).

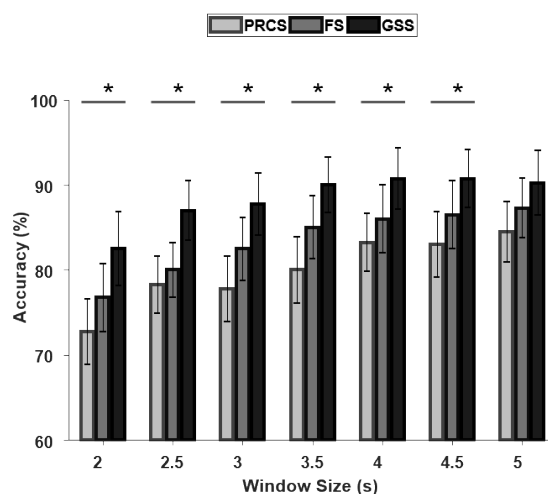


**FIGURE 5.** Comparison of the mean classification accuracy for the three stimuli in the AR environment when three individualized electrodes were used for each participant. Error bars indicate the standard errors across the participants. (\* represents Bonferroni-corrected  $p < 0.05$ ).

test indicated a statistical significance for all window sizes except 2 s (2 s:  $\chi^2 = 5.92$ ,  $p = 0.052$ ; 2.5 s:  $\chi^2 = 7.64$ ,  $p < 0.05$ ; 3 s:  $\chi^2 = 9.89$ ,  $p < 0.01$ ; 3.5 s:  $\chi^2 = 10.66$ ,  $p < 0.005$ ; 4 s:  $\chi^2 = 7.66$ ,  $p < 0.05$ ; 4.5 s:  $\chi^2 = 6.03$ ,  $p < 0.05$ ; 5 s:  $\chi^2 = 7.09$ ,  $p < 0.05$ ). The Wilcoxon signed rank post-hoc test with Bonferroni correction showed that the classification accuracy for GSS was significantly higher than that for PRCS for all window sizes in which the Friedman test showed a statistical significance (2.5 s:  $p < 0.05$ ; 3 s:  $p < 0.05$ ; 3.5 s:  $p < 0.05$ ; 4 s:  $p < 0.05$ ; 4.5 s:  $p < 0.05$ ; 5 s:  $p < 0.05$ ). No statistically significant difference was found between the other pairs.

Figure 5 illustrates the classification accuracy for each stimulus type when the three individually best electrodes were utilized. As shown in the figure, the performance was clearly improved in all three cases, whereas the overall trends did not change compared to the results shown in Fig. 4. The Friedman test indicated a statistical significance for all window sizes except 5 s (2 s:  $\chi^2 = 6.49$ ,  $p < 0.05$ ; 2.5 s:  $\chi^2 = 9.11$ ,  $p < 0.05$ ; 3 s:  $\chi^2 = 9.58$ ,  $p < 0.01$ ; 3.5 s:  $\chi^2 = 11.22$ ,  $p < 0.005$ ; 4 s:  $\chi^2 = 7.26$ ,  $p < 0.05$ ; 4.5 s:  $\chi^2 = 6.64$ ,  $p < 0.05$ ; 5 s:  $\chi^2 = 5.77$ ,  $p = 0.056$ ). The Wilcoxon signed rank post-hoc test with Bonferroni correction showed that the classification accuracy for GSS was significantly higher than that for PRCS for all window sizes in which the Friedman test showed a statistical significance (2 s:  $p < 0.05$ ; 2.5 s:  $p < 0.05$ ; 3 s:  $p < 0.05$ ; 3.5 s:  $p < 0.05$ ; 4 s:  $p < 0.05$ ; 4.5 s:  $p < 0.05$ ). No statistically significant difference was found between the other pairs. Because GSS consistently demonstrated a better performance than the other stimuli in the AR environment, we adopted this as the visual stimulus in the following online experiments. The individually selected electrode locations are provided in Table S1 included in the Supplementary Information file.

To confirm the extent to which the use of an AR display reduces the overall performance of SSVEP-based BCI compared to the conventional LCD-based SSVEP-BCI,

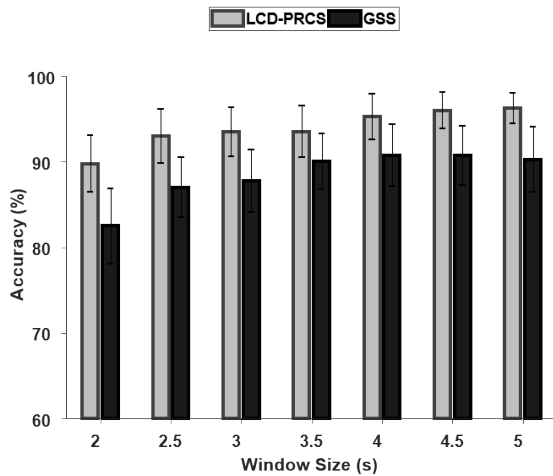


**FIGURE 6.** Comparison of the mean classification accuracies for LCD-PRCS and GSS. Error bars indicate the standard errors across the participants. Note that the performance was calculated by using the individualized electrode configuration.

we also compared the classification accuracy for GSS with that of a conventional checkerboard visual stimulus presented on an LCD monitor (Fig. 6). Whereas the performance of LCD-PRCS was consistently stronger than that of GSS for all window sizes (the average difference is less than 5%), there was no statistically significant difference. This result implies that the use of a see-through display to present visual stimuli somewhat degrades the overall performance of SSVEP-based BCI, but this degradation may not be sufficient to prevent utilization in practical scenarios.

To determine the optimal duration of the stimulus presentation, we evaluated the ITR and the classification accuracy with respect to different window sizes when GSS was employed with the universal and individual electrode configurations (Fig. 7). Before determining the optimal duration, we first tested whether there is a statistically significant difference between the performances for the universal and individualized electrode configurations using the Wilcoxon signed rank test. As shown in Fig. 7, the individually chosen electrode configurations outperformed the universal electrode configuration in terms of both the classification accuracy and ITR for many window sizes (Bonferroni-corrected  $p < 0.05$ ).

We selected 2.5 s as the optimal duration for stimulus presentation, based on the following observations: (i) Because the ITR is inversely proportional to the window size, a shorter window size yields a higher ITR. (ii) Although a 2 s window size corresponded to the highest ITR, the accuracy for the 2 s window was only 82.5%. In contrast, the accuracy for the 2.5 s window size was sufficiently high (87.0%), even being comparable to the accuracy for the 4 s window size (90.8%). Note that the accuracy was almost saturated above the 4 s window size.

Through this offline experiment, we confirmed that GSS might be the optimal visual stimulus for SSVEP-based BCI in an AR environment. In addition, we also confirmed that

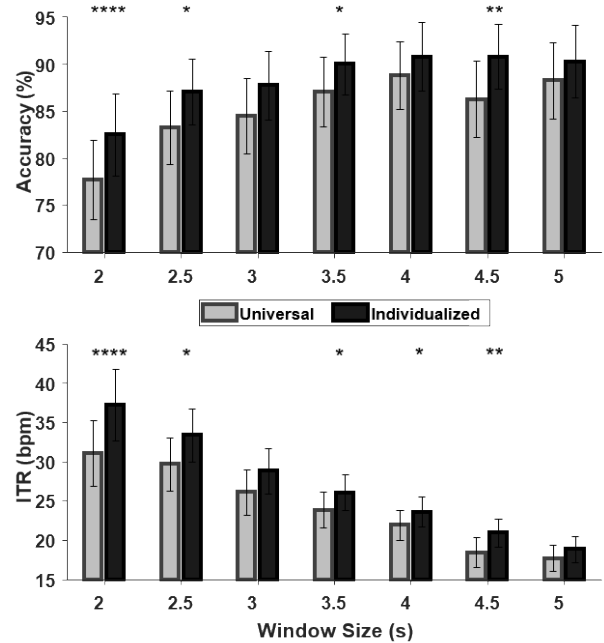


**FIGURE 7.** Comparison of the mean classification accuracy and information transfer rate (ITR) calculated with universal and individualized electrode configurations for GSS with different window sizes. Error bars indicate the standard errors across the participants (\* $p < 0.05$ , \*\* $p < 0.01$ , \*\*\*\* $p < 0.001$ , Wilcoxon signed rank test, Bonferroni-corrected).

adopting the individualized electrode configurations could result in a better performance, as already frequently reported in previous SSVEP studies [5], [37], [38]. Therefore, we utilized the individualized electrode configurations for each participant in the online experiments. The raw EEG datasets are available at [39].

### B. EXPERIMENT II – ONLINE HOME APPLIANCE CONTROL

Table 2 shows the classification accuracy and ITR achieved for each participant in the online home appliance control experiments (Experiment II). The total number of trials indicates the number of trials each participant completed in both the single-command and multicommand sessions. Each participant completed a different number of trials, because the number of errors occurring during the experiments was different for each participant. The accuracy was evaluated as (the number of correct trials) / (the number of total trials). The average accuracy and ITR were 92.8% and 37.4 bits/min, respectively. In addition, the efficiency values were close to 1 in all participants, demonstrating that the proposed smart home system has a potential to be utilized in practical scenarios.

The performance obtained in this study surpassed the best results previously reported in the literature on BCI in an AR environment [17], [18], [40]. There was no significant difference between the performance in the offline experiment (Experiment I) with individualized electrode configurations and in the online experiment (Experiment II) in terms of either the classification accuracy ( $p = 0.73$ ) or ITR

**TABLE 2. The experimental results in Experiment II.**

Subject	Correct Trials	Incorrect Trials	Accuracy (%)	ITR (bits/min)	Efficiency
P1	39	0	100	48	1
P2	40	4	90.9	34.0	0.86
P3	40	4	90.9	34.0	0.89
P4	42	3	93.3	37.0	0.89
P5	39	0	100	48	1
P6	39	0	100	48	1
P7	43	7	86.0	28.7	0.74
P8	41	7	85.4	28.1	0.85
P9	41	3	93.2	36.8	0.90
P10	39	1	97.5	43.0	0.96
P11	41	2	95.4	39.7	0.91
P12	42	6	87.5	30.2	0.81
P13	39	0	100	48	1
P14	40	1	97.6	43.1	0.95
P15	41	8	83.7	26.4	0.78
P16	42	3	93.3	37.0	0.87
P17	46	9	83.6	26.3	0.67
<b>Mean</b>			<b>92.8±5.9</b>	<b>37.4±7.9</b>	<b>0.89±0.10</b>

( $p = 0.84$ ), as assessed by the Wilcoxon signed rank test (Bonferroni-corrected).

Table 3 shows the average time required to switch the control system on or off using the eye-blink-based switch and the FPR (false operation) of the switch for each participant. All participants were able to switch the system on/off within 3 s, and the average time required to switch the system on/off was 2.6 s. Fifteen of the 17 participants exhibited an FPR of zero, whereas only two participants showed false positives. The average FPR was 0.015 times/min, or 0.891 times/h. These experimental results suggest that the proposed home appliance control BCI system could be utilized as a practical system. A video clip illustrating the home appliance control experiments is attached to this manuscript as a supplementary movie file (or visit [30] for higher quality video). All the online EEG raw datasets can be downloaded at [39].

#### IV. DISCUSSION

With the outstanding advances in medicine, healthcare, and therapeutics, life expectancy is gradually increasing, and thus the social burden of caring for elderly and paralyzed people will soon become serious [41], [42]. The smart home system

**TABLE 3. The performance of eye blink-based switch in Experiment II.**

Subject	Time elapsed to switch on/off (s)	FPR (times/min)	FPR (times/hour)
P1	2.4	0	0
P2	2.7	0	0
P3	2.7	0	0
P4	2.4	0	0
P5	2.6	0	0
P6	2.6	0	0
P7	2.6	0.168	10.100
P8	2.3	0.084	5.049
P9	2.9	0	0
P10	2.7	0	0
P11	2.2	0	0
P12	2.3	0	0
P13	3.3	0	0
P14	2.4	0	0
P15	2.6	0	0
P16	2.4	0	0
P17	2.7	0	0
<b>Mean</b>	<b>2.6±0.3</b>	<b>0.015±0.045</b>	<b>0.89±2.67</b>

could provide a plausible solution to circumvent this problem. In the present study, to develop a smart home system for home appliance control that can be utilized in real-world scenarios, we combined AR, IoT, and BCI technology. The proposed AR-BCI-IoT-based home appliance control system has a number of advantages over conventional smart home systems, in that (i) the user is not required to stay in a specific space to control a device as long as the device is connected to a network; (ii) the user does not have to move any part of their body to operate home appliances; and (iii) most importantly, the user can manipulate the system totally independently, without help from others. In the first offline study, we compared three different types of visual stimuli presented on an AR display to determine the optimal visual stimulus to achieve the best performance for SSVEP-based BCI. This has not been performed in any previous AR-based BCI studies. Based on the offline experimental results, we developed an online home appliance control system that can be operated solely by a user, who wears AR glasses. The experimental results demonstrated that the proposed BCI-based home appliance control system can be utilized in practical scenarios.

The results of our offline experiments showed that the mean accuracy of experiments with a stimulus on an LCD monitor (LCD-PRCS) was consistently higher than that for experiments with a stimulus on an AR-HMD display (PRCS, FS, and GSS). Even the same types of stimulus (PRCS) exhibited large differences of over 20% in the classification accuracy for a certain window size. This large degradation in the BCI performance may originate from the differences between the intrinsic properties of an AR display and LCD monitor. Unlike the LCD monitor, visual stimuli on an AR display are overlaid on the surrounding scenes, disturbing the user's concentration on the visual stimuli. In addition, the luminance change, or contrast of a visual stimulus is not as clear as on an LCD monitor, which might also affect the intensities of the SSVEP responses. A similar performance degradation was also reported in a previous study on a P300-based BCI in an AR environment [18]. For this reason, we needed to introduce a new visual stimulus to improve the overall performance of the SSVEP-based BCI system in an AR environment. Our experimental studies showed that the use of GSS as the visual stimulus for SSVEP-based BCI could enhance the performance of our AR-BCI-IoT-based home appliance control system to a level in which there was no significant difference from the conventional LCD-based stimulus presentation system.

Because GSS consistently exhibited the best performance among the three tested visual stimuli in an AR environment, it was selected as the visual stimulus in the online experiments. Considering that an AR display has a lower contrast and clearness than an LCD monitor, it is thought that GSS exhibited a better performance than the others on the AR display because GSS not only relies on luminance changes to elicit SSVEP responses, but also relies on motion. This differs from the conventional PRCS and FS, which rely solely on luminance changes to elicit SSVEP responses. Our results suggest that new visual stimuli effectively eliciting so-called "SSMVEP" or motion-related visual evoked potential (mVEP) might be developed in future studies to further enhance the performance of AR-based BCI.

In the online experiments, although no statistical significance was observed, the mean accuracy was improved by 5.8% compared to the offline experiments. This improvement might be a result of the following two factors: (i) The participants were accustomed to the visual stimuli via the repetitive experimental sequences, as shown in a previous study [43]. (ii) In contrast to the offline experiment, where no feedback on the classification results was provided to the participants, in the online experiment immediate feedback (i.e., operation of home appliances) was available to the participants. A similar phenomenon has frequently been reported in previous BCI studies [44]–[46].

Most BCI studies on the control of external devices such as robots, wheelchairs, and home appliances, have used LCD monitors to present visual stimuli [11], [12], [47]. Only a few studies attempted to use an AR-HMD to present the visual stimuli [17], [18], [48]. However, to the best of our knowledge

this is the first study to realize a practical home appliance control system by combining AR, IoT, and BCI technologies. Most importantly, our system outperformed all previously reported external device control systems that employed HMD as a rendering device (Table 4).

**TABLE 4. Comparison of performances with previous BCI-based external device control studies.**

Study	Accuracy (%)	ITR (bits/min)	Necessity of Calibration	Rendering Device
Kishore et al. [56]	87	24.7	Y	VR-HMD
Takano et al. [18]	79.4	5.4	Y	AR-HMD
Wang et al. [48]	83.3	4.6	Y	AR-HMD
Si-Mohammed et al. [17]	90	8.7	Y	AR-HMD
Proposed System	92.8	37.4	N	AR-HMD

In spite of the recent advancements of information and communication technologies, EEG-based BCIs have not been incorporated with practical home automation systems because the conventional EEG-based BCIs did not show high performance and were not convenient to use. In this study, we tried to overcome the limitations of the previous BCIs by combining AR-HMD and IoT technology with the SSVEP-based BCI. With AR-HMD, the BCI users do not need to carry any display device. In addition, using the IoT technology, the users can control external devices that are out of their sight. For example, the users of our smart home system can lock the front door or turn on a robotic vacuum located in a living room, even when they are lying on a bed or staying in a bathroom. In particular, it is expected that the proposed AR-BCI-IoT-based home appliance control system can provide the elderly and paralyzed people with freedom from being cared for, thereby elevating their quality of life.

In comparison with the existing assistive technologies including eye tracker and tongue switch, the proposed AR-BCI-IoT system has many advantages: (i) Most of the existing assistive technologies require calibration procedure to train a classifier, but our system does not require any calibration session. Although we individually selected an electrode set to enhance the performance of the system, the classification accuracy with a universal electrode set (O1, Oz, and O2) also showed an accuracy high enough to be employed for practical home appliance control (see Fig. 7). (ii) Our home appliance control system provides the user with more flexibility than the other assistive technologies. Thanks to the AR-HMD device and IoT technology, our system is not restricted by space as long as the device is connected to a

wireless network. To date, most of the assistive technologies have employed a “bulky” LCD monitor as a rendering device to present visual stimuli, markers, instructions, and visual feedbacks. Using a wearable see-through HMD, the users do not have to stay at a specific place any more. (iii) The conventional assistive technologies including eye-tracker and tongue switch also have some limitations. For example, the performance of camera-based eye trackers can be affected by the ambient light. Users of tongue switches might feel unpleasant and uncomfortable because of the attachment of sensors on the tongue. (iv) Some patients with severe paralysis, such as patients with severe amyotrophic lateral sclerosis (ALS), might lose the ability of controlling their eyeballs or tongue muscles, making it difficult to use eye-trackers or tongue switch. There have been a number of studies reporting that late stage ALS patients who cannot use eye tracker systems could successfully use SSVEP-based BCI systems [49]–[51]. In addition, the SSVEP-based BCI system implemented in this study can be readily extended to a system with a larger number of classes (even up to 30) [6], while it might not be easy to increase the number of classes in the conventional assistive technologies based on eye-tracker, EOG switch, and tongue switch.

With the rapid advances in information and communication technology, BCIs in AR and VR environments have begun to be explored in recent years. Previous studies have demonstrated that AR/VR-based BCIs have considerable potential to be utilized in a variety of application fields, such as entertainment [52], education [53], medicine [54], military [55], robotics [17], [56], health care [53], and home automation [18]. Considering that modern AR and VR devices are becoming more lightweight and easy to wear and are being actively incorporated with EEG devices (e.g., Neurable Inc., <http://www.neurable.com>), these technologies are likely to be commercialized in the near future. Lastly, in our future study, the usability of our system would be tested with the elderly and people with disabilities including patients with ALS. In addition, we will try to increase the overall performance of the proposed system by employing recently developed algorithms for the classification of SSVEP responses [57]–[59].

## REFERENCES

- [1] J. J. Vidal, “Toward direct brain-computer communication,” *Annu. Rev. Biophys. Bioeng.*, vol. 2, no. 1, pp. 157–180, Jun. 1973.
- [2] J. Wolpaw, N. Birbaumer, D. McFarland, G. Pfurtscheller, and T. Vaughan, “Brain-computer interfaces for communication and control,” *Clin. Neurophys.*, vol. 113, no. 6, pp. 767–791, Jun. 2002.
- [3] G. Dornhege, J. D. R. Millan, T. Hinterberger, D. J. McFarland, and K.-R. Müller, *Toward Brain-Computer Interfacing*. Cambridge, MA, USA: MIT Press, 2007, pp. 31–42.
- [4] N. Birbaumer, N. Ghanayim, T. Hinterberger, I. Iversen, B. Kotchoubey, A. Kübler, J. Perelmouter, E. Taub, and H. Flor, “A spelling device for the paralysed,” *Nature*, vol. 398, no. 6725, pp. 297–298, Mar. 1999.
- [5] H.-J. Hwang, J.-H. Lim, Y.-J. Jung, H. Choi, S. W. Lee, and C.-H. Im, “Development of an SSVEP-based BCI spelling system adopting a QWERTY-style LED keyboard,” *J. Neurosci. Methods*, vol. 208, no. 1, pp. 59–65, Jun. 2012.
- [6] X. Chen, Y. Wang, M. Nakanishi, X. Gao, T.-P. Jung, and S. Gao, “High-speed spelling with a noninvasive brain-computer interface,” *Proc. Nat. Acad. Sci. USA*, vol. 112, no. 44, pp. E6058–E6067, Oct. 2015.
- [7] C.-H. Han, Y.-W. Kim, D. Y. Kim, S. H. Kim, Z. Nenadic, and C.-H. Im, “Electroencephalography-based endogenous brain-computer interface for online communication with a completely locked-in patient,” *J. Neuroeng. Rehabil.*, vol. 16, no. 1, Jan. 2019, Art. no. 18.
- [8] B. H. Dobkin, “Brain-computer interface technology as a tool to augment plasticity and outcomes for neurological rehabilitation,” *J. Physiol.*, vol. 579, no. 3, pp. 637–642, Nov. 2007.
- [9] G. Pfurtscheller, G. R. Müller-Putz, R. Scherer, and C. Neuper, “Rehabilitation with brain-computer interface systems,” *Computer*, vol. 41, no. 10, pp. 58–65, Oct. 2008.
- [10] I. Martišius and R. Damaševičius, “A prototype SSVEP based real time BCI gaming system,” *Comput. Intell. Neurosci.*, vol. 2016, pp. 18–32, Mar. 2016.
- [11] G. Edlinger, C. Holzner, and C. Guger, “A hybrid brain-computer interface for smart home control,” in *Proc. Int. Conf. Hum.-Comput. Interact.*, Berlin, Germany, 2011, pp. 417–426.
- [12] C.-C. Lo, T.-Y. Chien, J.-S. Pan, and B.-S. Lin, “Novel non-contact control system for medical healthcare of disabled patients,” *IEEE Access*, vol. 4, pp. 5687–5694, 2016.
- [13] J. R. Wolpaw and D. J. McFarland, “Control of a two-dimensional movement signal by a noninvasive brain-computer interface in humans,” *Proc. Nat. Acad. Sci. USA*, vol. 101, no. 51, pp. 17849–17854, Dec. 2004.
- [14] T. O. Zander, L. R. Krol, N. P. Birbaumer, and K. Gramann, “Neuroadaptive technology enables implicit cursor control based on medial prefrontal cortex activity,” *Proc. Nat. Acad. Sci. USA*, vol. 113, no. 52, pp. 14898–14903, Dec. 2016.
- [15] E. Keeler, J. M. Guralnik, H. Tian, R. B. Wallace, and D. B. Reuben, “The impact of functional status on life expectancy in older persons,” *J. Gerontol., A*, vol. 65A, no. 7, pp. 727–733, Apr. 2010.
- [16] V. Bengtson, *Global Aging and Challenges to Families*. New York, NY, USA: Routledge, 2018, pp. 1–24.
- [17] H. Si-Mohammed, J. Petit, C. Jeunet, F. Argelaguet, F. Spindler, A. Évain, N. Roussel, G. Casiez, and A. Lécuyer, “Towards BCI-based interfaces for augmented reality: Feasibility, design and evaluation,” *IEEE Trans. Vis. Comput. Graphics*, to be published.
- [18] K. Takano, N. Hata, and K. Kansaku, “Towards intelligent environments: An augmented reality-brain-machine interface operated with a see-through head-mount display,” *Front. Neurosci.*, vol. 5, p. 60, Apr. 2011.
- [19] J. R. Wolpaw, H. Ramoser, D. J. McFarland, and G. Pfurtscheller, “EEG-based communication: Improved accuracy by response verification,” *IEEE Trans. Rehabil. Eng.*, vol. 6, no. 3, pp. 326–333, Sep. 1998.
- [20] P. Martinez, H. Bakardjian, and A. Cichocki, “Fully online multicommand brain-computer interface with visual neurofeedback using SSVEP paradigm,” *Comput. Intell. Neurosci.*, vol. 2007, pp. 1–9, Dec. 2007.
- [21] Y.-H. Lee, T. Zhan, and S.-T. Wu, “Prospects and challenges in augmented reality displays,” *Virtual Reality Intell. Hardware*, vol. 1, no. 1, pp. 10–20, Feb. 2019.
- [22] A. Duszyk, M. Bierzynska, Z. Radzikowska, P. Milanowski, R. Kus, P. Suffczynski, M. Michalska, M. Labecki, P. Zwolinski, and P. Durka, “Towards an optimization of stimulus parameters for brain-computer interfaces based on steady state visual evoked potentials,” *PLoS ONE*, vol. 9, no. 11, Nov. 2014, Art. no. e112099.
- [23] B. Allison, T. Lüth, D. Valbuena, A. Teymourian, I. Volosyak, and A. Gräser, “BCI demographics: How many (and what kinds of) people can use an SSVEP BCI?” *IEEE Trans. Neural Syst. Rehabil. Eng.*, vol. 18, no. 2, pp. 107–116, Apr. 2010.
- [24] E. C. Lalor, S. P. Kelly, C. Finucane, R. Burke, R. Smith, R. B. Reilly, and G. McDarby, “Steady-state VEP-based brain-computer interface control in an immersive 3D gaming environment,” *EURASIP J. Appl. Signal Process.*, vol. 2005, no. 19, pp. 3156–3164, Dec. 2005.
- [25] D. Zhu, J. Bieger, G. G. Molina, and R. M. Aarts, “A survey of stimulation methods used in SSVEP-based BCIs,” *Comput. Intell. Neurosci.*, vol. 2010, pp. 1–12, Jan. 2010.
- [26] M. Nakanishi, Y. Wang, Y.-T. Wang, Y. Mitsukura, and T.-P. Jung, “Generating visual flickers for eliciting robust steady-state visual evoked potentials at flexible frequencies using monitor refresh rate,” *PLoS ONE*, vol. 9, no. 6, Jun. 2014, Art. no. e99235.
- [27] Y. Punsawad and Y. Wongsawat, “Motion visual stimulus for SSVEP-based BCI system,” in *Proc. Annu. Int. Conf. IEEE Eng. Med. Biol. Soc.*, San Diego, CA, USA, Aug./Sep. 2012, pp. 3837–3840.
- [28] J. Xie, G. Xu, J. Wang, F. Zhang, and Y. Zhang, “Steady-state motion visual evoked potentials produced by oscillating Newton’s rings: Implications for brain-computer interfaces,” *PLoS ONE*, vol. 7, no. 6, Jun. 2012, Art. no. e39707.

- [29] W. Yan, G. Xu, M. Li, J. Xie, C. Han, S. Zhang, A. Luo, and C. Chen, "Steady-state motion visual evoked potential (SSMVEP) based on equal luminance colored enhancement," *PLoS ONE*, vol. 12, no. 1, Jan. 2017, Art. no. e0169642.
- [30] *A Youtube Video Entitled Development of an Online Home Appliance Control System Using Augmented Reality and SSVEP-Based BCI*. [Online]. Available: <https://youtu.be/OnOAG3n1WwM>
- [31] D. Regan, "Steady-state evoked potentials," *J. Opt. Soc. Amer.*, vol. 67, no. 11, pp. 1475–1489, Nov. 1977.
- [32] H. Bakardjian, T. Tanaka, and A. Cichocki, "Optimization of SSVEP brain responses with application to eight-command brain-computer interface," *Neurosci. Lett.*, vol. 469, pp. 34–38, Jan. 2010.
- [33] *The Cogent Project*. [Online]. Available: <http://www.vislab.ucl.ac.uk/cogent.php>
- [34] *What is the Function of the CMS and DRL Electrodes. Ground, Reference or What?*. [Online]. Available: <http://www.biosemi.com/faq/cms&drl.htm>
- [35] Y. Zhang, D. Guo, D. Yao, and P. Xu, "The extension of multivariate synchronization index method for SSVEP-based BCI," *Neurocomputing*, vol. 269, pp. 226–231, Dec. 2017.
- [36] W.-D. Chang, J.-H. Lim, and C.-H. Im, "An unsupervised eye blink artifact detection method for real-time electroencephalogram processing," *Physiol. Meas.*, vol. 37, no. 3, pp. 401–417, Feb. 2016.
- [37] Y. Wang, R. Wang, X. Gao, B. Hong, and S. Gao, "A practical VEP-based brain-computer interface," *IEEE Trans. Neural Syst. Rehabil. Eng.*, vol. 14, no. 2, pp. 234–240, 2006.
- [38] O. Friman, I. Volosyak, and A. Graser, "Multiple channel detection of steady-state visual evoked potentials for brain-computer interfaces," *IEEE Trans. Biomed. Eng.*, vol. 54, no. 4, pp. 742–750, Apr. 2007.
- [39] *Raw Data Used for the Development of an Online Home Appliance Control System Using Augmented Reality and SSVEP-Based Brain-Computer Interface*. [Online]. Available: <https://figshare.com/s/ad6ebd0786a46fd38ec3>
- [40] J. Faller, B. Z. Allison, C. Brunner, R. Scherer, D. Schmalstieg, G. Pfurtscheller, and C. Neuper, "A feasibility study on SSVEP-based interaction with motivating and immersive virtual and augmented reality," 2017, *arXiv:1701.03981*. [Online]. Available: <https://arxiv.org/abs/1701.03981>
- [41] M. Sato, "Expanding welfare concept and assistive technology," in *Proc. IEK Annu. Fall Conf.*, 2000, pp. 156–161.
- [42] D. H. Stefanov, Z. Bien, and W.-C. Bang, "The smart house for older persons and persons with physical disabilities: Structure, technology arrangements, and perspectives," *IEEE Trans. Neural Syst. Rehabil. Eng.*, vol. 12, no. 2, pp. 228–250, Jun. 2004.
- [43] C. Vidaurre, A. Schlogl, R. Cabeza, R. Scherer, and G. Pfurtscheller, "A fully on-line adaptive BCI," *IEEE Trans. Biomed. Eng.*, vol. 53, no. 6, pp. 1214–1219, Jun. 2006.
- [44] C. Vidaurre and B. Blankertz, "Towards a cure for BCI illiteracy," *Brain Topogr.*, vol. 23, no. 2, pp. 194–198, Jun. 2010.
- [45] A. Ramos-Murguialday, M. Schürholz, V. Caggiano, M. Wildgruber, A. Caria, E. M. Hammer, S. Halder, N. Birbaumer, "Proprioceptive feedback and brain computer interface (BCI) based neuroprostheses," *PLoS ONE*, vol. 7, no. 10, Oct. 2012, Art. no. e47048.
- [46] E. Tidoni, P. Gergondet, A. Kheddar, and S. M. Aglioti, "Audio-visual feedback improves the BCI performance in the navigational control of a humanoid robot," *Frontiers Neurobot.*, vol. 8, p. 20, Jun. 2014.
- [47] K. Kansaku, N. Hata, and K. Takano, "My thoughts through a robot's eyes: An augmented reality-brain-machine interface," *Neurosci. Res.*, vol. 66, no. 2, pp. 219–222, Oct. 2010.
- [48] M. Wang, R. Li, R. Zhang, J.-H. Lee, G. Li, and D. Zhang, "A wearable SSVEP-based BCI system for quadcopter control using head-mounted device," *IEEE Access*, vol. 6, pp. 26789–26798, 2018.
- [49] H.-J. Hwang, C.-H. Han, J.-H. Lim, Y.-W. Kim, S.-I. Choi, K.-O. An, J.-H. Lee, H.-S. Cha, S. H. Kim, and C.-H. Im, "Clinical feasibility of brain-computer interface based on steady-state visual evoked potential in patients with locked-in syndrome: Case studies," *Psychophysiology*, vol. 54, no. 3, pp. 444–451, Dec. 2017.
- [50] J. H. Lim, Y.-W. Kim, J.-H. Lee, K.-O. An, H.-J. Hwang, H.-S. Cha, C.-H. Han, and C.-H. Im, "An emergency call system for patients in locked-in state using an SSVEP-based brain switch," *Psychophysiology*, vol. 54, no. 11, pp. 1632–1643, Jul. 2017.
- [51] D. Lesenfants, D. Habbal, Z. Lugo, M. Lebeau, P. Horki, E. Amico, C. Pokorny, F. Gómez, A. Soddu, G. Müller-Putz, S. Laureys, and Q. Noirhomme, "An independent SSVEP-based brain-computer interface in locked-in syndrome," *J. Neural Eng.*, vol. 11, no. 3, 2014, Art. no. 035002.
- [52] A. Lecuyer, F. Lotte, R. B. Reilly, R. Leeb, M. Hirose, and M. Slater, "Brain-computer interfaces, virtual reality, and videogames," *Computer*, vol. 41, no. 10, pp. 66–72, Oct. 2008.
- [53] P. Gang, J. Hui, S. Stirenko, Y. Gordienko, T. Shemsedinov, O. Alienin, Y. Kochura, N. Gordienko, A. Rojbi, J. R. L. Benito, and E. González, "User-driven intelligent interface on the basis of multimodal augmented reality and brain-computer interaction for people with functional disabilities," in *Proc. Future Inf. Commun. Conf.*, Singapore, 2017, pp. 612–631.
- [54] H. Si-Mohammed, F. Argelaguet, G. Casiez, N. Roussel, and A. Lécuyer, "Brain-computer interfaces and augmented reality: A state of the art," in *Proc. 7th Graz Brain-Comput. Interface Conf.*, Graz, Austria, 2017, pp. 1–7.
- [55] M. Mekni and A. Lemieux, "Augmented reality: Applications, challenges and future trends," in *Proc. 13th Int. Conf. Appl. Comput. Appl. Comput. Sci. (ACACOS)*, Kuala Lumpur, Malaysia, 2014, pp. 23–25.
- [56] S. Kishore, M. González-Franco, C. Hintemüller, C. Kapeller, C. Guger, M. Slater, and K. J. Blom, "Comparison of SSVEP BCI and eye tracking for controlling a humanoid robot in a social environment," *Presence, Teleoperators Virtual Environ.*, vol. 23, no. 3, pp. 242–252, Oct. 2014.
- [57] E. Yin, Z. Zhou, J. Jiang, Y. Yu, and D. Hu, "A dynamically optimized SSVEP brain-computer interface (BCI) speller," *IEEE Trans. Biomed. Eng.*, vol. 62, no. 6, pp. 1447–1456, Jun. 2015.
- [58] J. Jiang, E. Yin, C. Wang, M. Xu, and D. Ming, "Incorporation of dynamic stopping strategy into the high-speed SSVEP-based BCIs," *J. Neural Eng.*, vol. 15, no. 4, Jun. 2018, Art. no. 046025.
- [59] Y. Zhang, E. Yin, F. Li, Y. Zhang, T. Tanaka, Q. Zhao, Y. Cui, P. Xu, D. Yao, and D. Guo, "Two-stage frequency recognition method based on correlated component analysis for SSVEP-based BCI," *IEEE Trans. Neural Syst. Rehabil. Eng.*, vol. 26, no. 7, pp. 1314–1323, Jul. 2018.



**SEONGHUN PARK** received the B.S. degree from the Department of Biomedical Engineering, Hanyang University, South Korea, in 2015, where he is currently pursuing the Ph.D. degree. His current research interests include brain-computer interfaces, smart home systems, and biomedical signal processing.



**HO-SEUNG CHA** received the B.S. degree from the Department of Biomedical Engineering, Yonsei University, South Korea, in 2013, and the M.S. degree from Hanyang University, South Korea, in 2015, where he is currently pursuing the Ph.D. degree with the Department of Biomedical Engineering. His current research interests include machine learning, human computer interaction, and biomedical signal processing.



**CHANG-HWAN IM** (M'09) received the B.S. degree from the School of Electrical Engineering, Seoul National University, South Korea, in 1999, and the M.S. and Ph.D. degrees in 2001 and 2005, respectively. He was a Postdoctoral Associate with the Department of Biomedical Engineering, University of Minnesota, Minneapolis, USA, from 2005 to 2006. From 2006 to 2011, he was with the Department of Biomedical Engineering, Yonsei University, South Korea, as an Assistant/Associate

Professor. Since 2011, he has been with the Department of Biomedical Engineering, Hanyang University, South Korea, as a Full Professor. He is currently the Director of the Computational Neuroengineering Laboratory and Research Center for Neural Engineering, Hanyang University, South Korea. He has authored more than 160 articles in peer-reviewed international journals. His current research interests include neuroelectromagnetics and computational neuroengineering, especially brain-computer interfaces, diagnosis of neuropsychiatric diseases, noninvasive brain stimulation, and dynamic neuroimaging.